Environ. Sci. Technol. **2010,** *44,* 3908–3912

Precursors of Dichloroacetamide, an Emerging Nitrogenous DBP Formed during Chlorination or Chloramination

WEN-HAI CHU,[†] NAI-YUN GAO,*[,†] YANG DENG,[†] AND STUART W. KRASNER[§]

State Key Laboratory of Pollution Control and Resources Reuse, College of Environmental Science and Engineering, Tongji University, Shanghai, 200092, China, Department of Earth and Environmental Studies, Montclair State University, Montclair, New Jersey, 07043, and Metropolitan Water District of Southern California, 700 Moreno Avenue, La Verne, California 91750-3399

Received February 4, 2010. Revised manuscript received March 31, 2010. Accepted April 6, 2010.

Haloacetamides (HAcAms) are an emerging class of nitrogenous disinfection byproducts (N-DBPs). However, there is a limited understanding about the precursors of HAcAms. In this study, we screened the precursors of dichloroacetamide (DCAcAm), the most commonly identified HAcAm in chlorinated or chloraminated drinking water. DCAcAm formation potential (FP) of raw water samples collected in different months from a reservoir in China was determined during chlorination, and the highest DCAcAm FP typically occurred in the summer samples. Dissolved organic matter (DOM) in a representative summer raw water sample was separated into six fractions by a series of resin elutions. Among them, hydrophilic acid (HiA) DOM showed the maximum DCAcAm FP, followed by hydrophilic bases (HiB) and, to a much lower extent, hydrophobic acids (HoA). Fluorescence excitation−emission matrix (EEM) spectra revealed that a mass of protein-like substances in the HiA fraction, made up of amino acids (AAs), were the likely DCAcAm precursors. Finally, we investigated the DCAcAm yields of 20 AAs during chlorination. Among them, seven AAs (aspartic acid, histidine, tyrosine, tryptophan, glutamine, asparagine, phenylalanine) could form DCAcAm during chlorination, with the corresponding DCAcAm yields of 0.231, 0.189, 0.153, 0.104, 0.078, 0.058, and 0.050 mmol/mol AA.

Introduction

Chlorine and chloramines, two widely used low-cost disinfectants, can react with dissolved organic matter (DOM) in water to form disinfection byproducts (DBPs) of potential human health concern. Since the first discovery of DBPs in the early 1970s (*1*, *2*), DBPs have become one of the major driving forces in drinking water regulations, research, and water utility operations. The list of DBPs identified in treated drinking waters has grown from a few trihalomethanes (THMs) to a long list of halogenated and nonhalogenated organic or inorganic species (*3*, *4*). This list continues to expand with the improvement of the analytical techniques and the advancement in the knowledge of their toxicity (*5*–*8*). Over the last 30 years, most DBP studies have focused on the currently regulated DBPs (THMs and haloacetic acids [HAAs]) (*1*, *2*, *9*, *10*), leading to a better understanding of the toxicity, occurrence, formation, and control of THMs and HAAs than those of emerging unregulated DBPs, particularly nitrogenous DBPs (N-DBPs). N-DBPs are formed by the reactions between disinfectants and DOM, especially dissolved organic nitrogen (DON) compounds (*11*). Although they are present at a low level, N-DBPs may be more carcinogenic and mutagenic than the currently regulated DBPs (*12*, *13*).

Research on various N-DBPs (e.g., haloacetonitriles [HANs], halonitromethanes [HNMs], nitrosamines) have been reported (*14*–*17*). However, little is known about the formation of haloacetamides (HAcAms), an emerging class of N-DBPs. Five HAcAms (Supporting Information [SI] Figure S1) were identified and quantified at 12 drinking water treatment plants in the U.S. (*4*, *8*). Plewa et al. (*18*) reported that the HAcAms were 99×, 142×, 2×, and 1.4× more cytotoxic than 13 HAAs, 5 regulated HAAs, HANs, and HNMs, respectively. Moreover, they were 19×, 12×, and 2.2× more genotoxic than 13 HAAs, 5 regulated HAAs and HNMs, respectively.

A better understanding of the characteristics of HAcAm precursors in raw water is critical to the development of effective strategies to minimize HAcAm formation during chlorination. Unfortunately, the nature of DOM is not well understood, mostly due to their heterogeneity and complexity in chemical structure. Moreover, few studies have characterized the precursors for N-DBPs. Although some studies have suggested certain DON moieties of DOM as the likely precursors for N-DBPs (*16*, *19*, *20*), there has not been a study for the screening of specific nitrogenous compounds with high HAcAm formation potential (FP) in natural waters. In the 12-plant U.S. study (*8*), dichloroacetamide (DCAcAm) was present at the highest concentration (as high as 5.6 μg/L in the plant effluents) among the five HAcAms studied. These waterworks used a combination of chlorine and alternative disinfectants. Base-catalyzed hydrolysis of the commonly formed DBP dichloroacetonitrile (DCAN) can result in the formation of DCAcAm (*15*). Therefore, DCAcAm was used as a representative model HAcAm in this study. Our major goal was to screen the main DCAcAm precursors by investigating the DCAcAm FP of different DOM fractions in raw water during chlorination or chloramination, analyzing the characteristics of the high-FP fractions by spectroscopic techniques, and examining DCAcAm yields of 20 amino acids (AAs) during chlorination (pH 7.5, AA concentration = 50 μmol/L, molar ratio of chlorine as Cl to AAs as N [Cl/N] = 4:1).

Experimental Section

Experimental Procedures. Samples were collected in April−December, 2009 from the intake of a waterworks whose source was the Qingcaosha Reservoir. The reservoir is located in the estuary of the Yangtze River, the longest river in China, and supplies 7.19×10^7 m^3/d source water to meet the drinking water demand of ~10 million people in Shanghai. Once collected, the sample was immediately filtered through a prerinsed 0.7 μm glass filter membrane (GF/F, 0.7 μm, Whatman, UK) and was stored in the dark at 4 °C until used. The DBPFP of the water sample was determined on the same day as the sample collection; whereas the DOM fractionation was finished within a couple of days of sample collection. Analysis of the raw water samples did not show a detectable

* Corresponding author.
[†] Tongji University.
[†] Montclair State University.
[§] Metropolitan Water District of Southern California.

10.1021/es100397x

Published on Web 04/16/2010

DCAcAm background level. To screen the DCAcAm precursors, DCAcAm FP was determined under controlled laboratory conditions with chlorination. After comparing the DCAcAm yields in different months, FP experiments were conducted with solutions containing different DOM fractions (hydrophilic acids, HiA; hydrophobic acids, HoA; hydrophilic bases, HiB; hydrophobic bases, HoB; hydrophilic neutrals, HiN; hydrophobic neutrals, HoN) of raw water samples collected in the month with the highest DCAcAm yield. To determine the characteristics of the DCAcAm precursors, the isolated fractions were analyzed by 3-D fluorescence and UV/vis spectrophotometry. In addition, DCAcAm yields of 20 AAs during chlorination were evaluated.

Fractionation and Characterization of DOM. Various DOM isolates, including hydrophilic and hydrophobic acid, base, and neutral fractions, were obtained from the samples by using the XAD-8/MSC/A7 resin procedure (SI Figure S2) based on the methods developed by Leenheer (*21*), Imai et al. (*22*), and Zhang et al. (*23*). By diluting each isolate, the DOC concentration of each fraction was adjusted to the same level (i.e., 4.0 mg/L).

Fluorescence spectra were recorded by a fluorescence spectrophotometer (model F-4500, Hitachi, Japan). Three-dimensional spectra were obtained by measuring the emission (Em) spectra in the range from 200 to 600 nm repeatedly, and at excitation wavelengths (Ex) from 200 to 600 nm, at 5 nm intervals in the excitation domain. The software MatLab 7.1 (MathWorks Inc., Natick, MA) was employed to process the excitation−emission matrix (EEM) data. Based on the EEM data, a fluorescence index (FI) can be calculated by the ratio of fluorescence intensity at emission 450 and 500 nm, at excitation 370 (*24*). A higher FI (>1.5) reflects organic matter of an autochthonous (microbial) origin, whereas a lower FI (<1.5) reflects organic matter of an allochthonous (terrestrial) origin.

Chlorination and Chloramination of DOM Isolates. A sodium hypochlorite solution (active chlorine >5%, Sinopharm Chemical Reagent Co., Ltd., China) was used to prepare free chlorine stock solutions. The DCAcAm FP tests were conducted using the methods developed by Krasner et al., using free chlorine and chloramines (*25, 26*). Solutions containing DOM fractions were chlorinated or chloraminated in sealed 50 mL amber glass bottles at 24 °C in the dark for 24 h or 3 days, respectively (*25–27*). Solution pH was buffered at pH 7 with phosphate salts (0.3-M sodium dihydrogen phosphate, NaH_2PO_4, and 0.2-M sodium monohydrogen phosphate, Na_2HPO_4) obtained from Sigma-Aldrich. The disinfectant dosages for FP tests were calculated by eq 1 for free chlorine (*25*) or eq 2−3 for chloramines (*26*). The free chlorine condition was achieved by addition of sufficient chlorine to break out any ammonia.

$$Cl_2\text{dosage(mg/L)} = 3 \times \text{DOC(mg-C/L)} + 7.6 \times NH_3\text{(mg-N/L)} + 10\text{(mg/L)} \quad (1)$$

$$Cl_2\text{dosage(mg/L)} = 3 \times \text{DOC(mg-C/L)} \quad (2)$$

Cl_2:NH_3-N = 3:1 weight ratio (ammonia added first, except as noted) (3)

Analytical Methods. DOC and total dissolved nitrogen (TDN) were measured by a TOC analyzer equipped with a TNM total nitrogen detection unit (Shimadzu TOC-V_{CPH}, Japan). The DON concentration was the difference in the measured TDN and dissolved inorganic nitrogen (DIN). DIN (ammonia, nitrate, and nitrite) were measured with a portable spectrophotometer (HACH DR2800, USA). UV absorption at 272 nm (UV_{272}) was determined with a UV/vis double-beam spectrophotometer (Unico4802, U.S.). The UV_{272} to DOC ratio ($SUVA_{272}$) was used to represent total organic halogen (TOX)

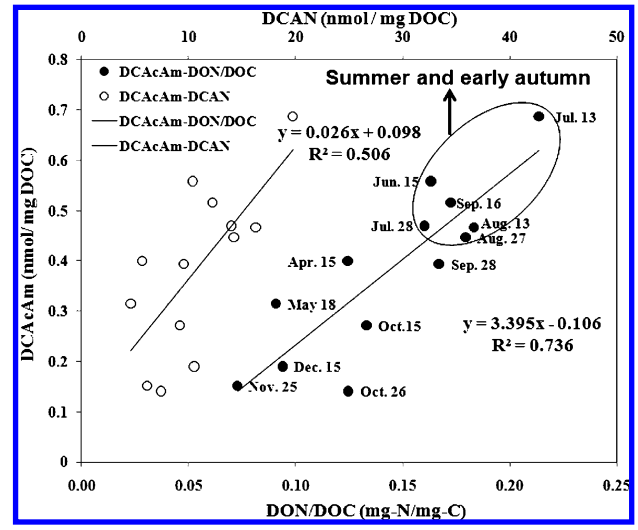

FIGURE 1. DCAcAm and DCAN yields during DBPFP test (chlorination) in different months (pH 7, raw water DOC = 3.84−6.33 mg/L).

formation resulting from chlorination (*28, 29*). Residual disinfectants were measured by the total and free DPD (*N,N*-diethyl-*p*-phenylenediamine) colorimetric method 4500-Cl (*30*). To stop the FP tests, the disinfectant residuals were quenched with ascorbic acid with normality twice as high as the initial normality of chlorine added. Glacial acetic acid was used to lower the pH to 4.8−5.5 for the THM and HAN samples, and to 5.0 ± 0.2 for the DCAcAm samples to prevent base-catalyzed hydrolysis of DCAN or DCAcAm (*31*). Chloroform (CF) and DCAN were analyzed with a gas chromatograph (GC) (Shimadzu-QP2010, Japan) with an electron capture detector (ECD), based on U.S. Environmental Protection Agency (USEPA) method 551.1. DCAcAm was analyzed using liquid−liquid extraction (LLE) and GC/mass spectrometry (MS) (Shimadzu-QP2010, Japan). The details of the DCAcAm analysis are available elsewhere (*31–33*) and are described in the Supporting Information.

Results and Discussions

Differences in DBP Yields in Different Months. Qingcaosha Reservoir water quality characteristics (e.g., DOC, DON, UV) are briefly described in SI Table S1. In the FP tests, the trichloroacetamide (TCAcAm) concentrations in most of the water samples were below the detection limit. In contrast, the DCAcAm levels in all of the samples were above the detection limit, as shown in Figure 1, with relative standard deviations ($n = 3$) of <6.0%. This observation motivated us to investigate and screen the precursors of DCAcAm.

The occurrence and variability in DCAcAm FP in different months are shown in Figure 1. In the DBPFP tests, we found somewhat of a linear relationship ($R^2 = 0.51$) between the two N-DBPs (Figure 1), which suggests similar precursors and/or mechanisms of formation. Moreover, we found a linear relationship between DCAcAm yield and DON/DOC ($R^2 = 0.74$) (Figure 1) and between DCAN yield and DON/DOC ($R^2 = 0.71$), the latter of which is in agreement with the finding of Reckhow et al. (*34*) (SI Figure S3). However, in the research of Reckhow and colleagues, they reported similar DCAN yields as in this study, but at lower DON/DOC ratios. These observations imply that a portion of the DON plays an essential role in the formation of DCAcAm and DCAN, where that portion is probably watershed-specific, and the presence of DON may act as an indicator (but not predictor per se) of N-DBP FP. As shown in Figure 1, DCAcAm and DCAN yields from June 15th through September 16th were higher than those in other times sampled, probably because the DCAcAm and DCAN precursors were much more

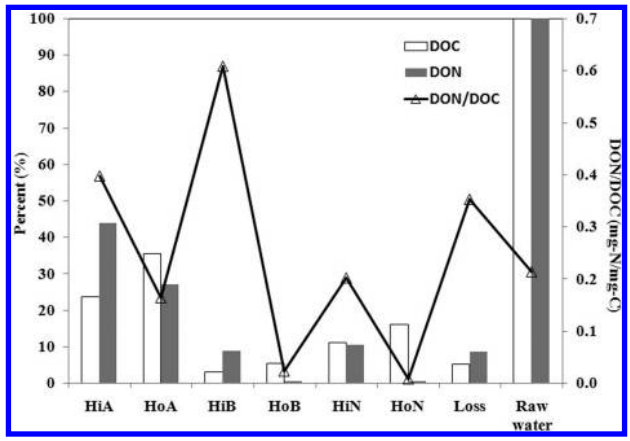

FIGURE 2. Distribution of DOC and DON of Qingcaosha Reservoir water in a representative summer water sample (collected on July 13, 2009).

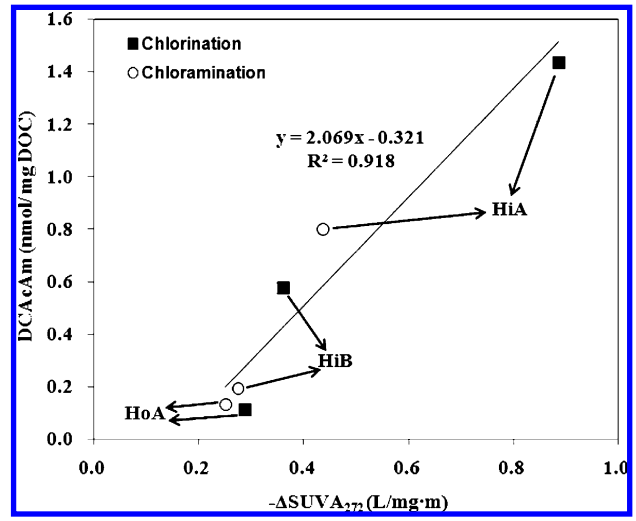

FIGURE 3. DCAcAm yield of different DOM isolates during DBPFP test (pH 7, DOC of each fraction = 4.0 mg/L; relative standard deviation of DCAcAm samples for HiA, HoA, and HiB fractions were 0.8, 5.7, and 1.8% during chlorination, and 1.5, 4.2, and 2.2% during chloramination).

abundant in summer and early autumn. Alternatively, there was no correlation between DCAcAm yield and that of chloroform (SI Figure S4). Likewise, Trehy et al. (*35*) studied chlorinated lake waters and chlorinated wastewater and reported that chloroform formation was independent of the formation of DCAN, suggesting different precursors for these chlorination byproducts (i.e., humic substances versus AAs or other nitrogenous substances).

Characteristics of DOM Isolates in Summer. Because the samples collected in summer and early autumn showed the highest FP for DCAcAm and DCAN, we fractionated the DOM of the July 13, 2009 sample into six fractions. The distribution of these fractions, in terms of DOC and DON, is shown in Figure 2. As seen, the overall acid fraction (HiA and HoA) was the dominant part of the DOC and DON, accounting for 59.1% of the total DOC and 68.2% of the total DON, respectively. Moreover, the hydrophobic fractions (HoA, HoB, and HoN) contributed to 57.1% of the DOC, whereas the hydrophilic fractions accounted for 60.5% of the total DON. Among the six individual fractions, HoA, primarily composed of humic and fulvic acids, was the largest fraction of the total DOC (35.5%) and the second major contributor to the total DON (26.1%). HiA was the second major contributor to the total DOC (23.6%) and the largest fraction of total DON (42.1%). The higher DON/DOC of HiA than that of HoA was probably because the HiA contained a mass of sugars and amino sugars (*36*). However, among all the fractions, HiB was the one with the highest DON/DOC (0.61 mg-N/mg-C). In each case, for the acids, bases or neutrals, the hydrophilic fraction was always higher in DON/DOC than the corresponding hydrophobic fraction. The observed distribution of DOM in Qingcaosha Reservoir water was similar with a previous study (*37*) on other reservoir waters (e.g., hydrophobic fractions accounted for 51−62% of total DOC), but was noticeably different from the typical values in river water samples (e.g., HoA only contributed 41−50% of total DOC). There were relatively small mass losses in total DOC (5.1%) and DON (12.6%), probably caused by the washing and elution of columns and volatilization during the rotary evaporation procedure.

DBP Yields of Different DOM Fractions. Figure 3 shows the DCAcAm yields of the different fractions, and presents their relationship to $-\Delta SUVA_{272}$ during two disinfection processes (chlorination and chloramination). No DCAcAm was detected in the HoB, HiN, and HoN isolates, indicating that these three fractions appeared not to contribute to the formation of DCAcAm. For both chlorination and chloramination, DCAcAm yields were the highest for the HiA isolates, followed by HiB, and then HoA. The four most N-poor isolates, that is, the ones with the lowest DON/DOC ratios (i.e., HoB, HiN, HoN, HoA) produced little or no DCAcAm, whereas the two most N-rich fractions (i.e., HiA, HiB) produced the most DCAcAm. Although HiA was less N-rich than HiB, it produced more DCAcAm. Therefore, it seems that the characteristics of the DON, rather than the amount of DON, influenced the yield of DCAcAm. Moreover, DCAcAm yields for HiA and HiB in the free chlorine FP tests were approximately twice as high as in the chloramine FP tests. However, for HoA, the DCAcAm yield during chlorination was almost the same as that during chloramination, albeit both were low (Figure 3). The different observations in DCAcAm formation indicate that different isolates might have different DCAcAm formation pathways during free chlorination and chloramination.

Additionally, Figure 3 shows a good linear relation between $-\Delta SUVA_{272}$ and DCAcAm yields during chlorination and chloramination of HiA, HiB, and HoA, which implies the possibility of estimating HAcAm formation by measuring the reduction in $SUVA_{272}$, although it is likely that the precise relationship will be dependent on source water quality. This figure suggests that DCAcAm yield correlated with the destruction of some of the aromaticity of the DOM. As shown below, some of the AAs with high DCAcAm yields have aromatic rings. We also investigated the relationship between DCAcAm yield and DON/DOC in SI Figure S5, where the yield was per unit DOC or per unit DON. In either case, HiA had the highest yield, even though it was not as N-rich as HiB. As discussed below, the different AAs tested had very different DCAcAm yields. The same is likely true for other components of the DON. Thus, HiA contained DON components that were more reactive in forming DCAcAm than HiB. Finally, we compared in SI Table S2 the DCAcAm yield of the raw water collected on July 13, 2009 with the weighted sum of the DCAcAm yields of each DOM fraction isolated from the raw water. The majority (60%) of the DCAcAM yield was accounted for by the different DOM fractions. This is discussed further in the Supporting Information.

Properties of Different DOM Isolates. EEM spectra were used to characterize different DOM fractions, as shown in SI Figure S6. According to the fluorescence regional integration (FRI) method developed by Chen and colleagues (*38*), the EEM spectra were operationally summarized into five regions, as shown in SI Figure S7. As shown in SI Figure S6 and Table 1, HiA showed the most intense peak (1363 mV) at Ex/Em of 280/320 nm, which fell within the soluble microbial product

TABLE 1. EEM Spectra Peaks of DOM Fractions

DOM fraction	Ex/Em (nm/nm)	substance	intensity (mV)	FI
HiA	280/320	SMP-like	1363.0	1.33
	230/330	aromatic proteins	604.5	
	320/440	humic acid-like	267.2	
HoA	240/350	aromatic proteins	555.5	1.30
	310/420	humic acid-like	343.2	
	240/430	fulvic acids-like	456.8	
HiB	290/370	SMP-like	271.6	2.23
	220/360	aromatic proteins	222.3	
HoB	240/355	aromatic proteins	210.0	2.60
HiN	310/480	humic acid-like	884.5	0.61
	250/500	fulvic acids-like	816.5	
HoN	240/410	fulvic acids-like	189.9	1.35

(SMP)-like region (λ_{ex} > 250 nm, λ_{em} < 380 nm), and the second-highest peak (604.5 mV) at Ex/Em of 230/330 nm within the aromatic protein region (λ_{ex} < 250 nm, λ_{em} < 380 nm), and the third highest peak (267.2 mV) at Ex/Em of 320/440 nm, a portion of the humic acid-like compound region (λ_{ex} > 250 nm, λ_{em} > 380 nm). HiB also had its most intense peak (271.6 mV) in the SMP-like region and its second highest peak (222.3 mV) in the aromatic protein region, but the peak intensities were significantly lower than those for HiA. HiN contained two distinct humic acid-like peaks and one distinct peak in the fulvic acid-like region (λ_{ex} < 250 nm, λ_{em} > 380 nm). The most humic acid-like peak intensity (884.5 mV) in HiN was significantly higher than that for HiA. Although HoA is typically associated with humic substances and it did have peaks in the humic and fulvic acid-like regions, the peaks were weak. Alternatively, HoA's largest peak was for the aromatic protein region.

No DCAcAm was detected during chlorination of the HiN fraction, suggesting that humic and fulvic acid-like substances were not DCAcAm precursors. Thus, the DCAcAm precursors associated with HoA, albeit present in a low yield, may have been due to aromatic proteins. HoA and HoB both had an aromatic protein peak, but only HoA produced DCAcAm during the FP test. This may have been due to different aromatic protein peak intensities. The aromatic protein peak intensity (555.5 mV) in the HoA EEM spectra was higher than that for HoB (210.0 mV). The aromatic protein peak intensity in the HoA EEM spectra was significantly higher than that for HiB (222.3 mV); however, HiB exhibited much higher DCAcAm FP than HoA. In addition, HiB contained an SMP-like peak, which may have contributed to its DCAcAm formation. HiA produced the most DCAcAm and its most intense peak was for the SMP-like substances. Moreover, HiA had more of this SMP-like peak and produced more DCAcAm than HiB. Thus, these data suggest that formation of DCAcAm was more attributed to SMP-like substances than aromatic proteins.

From Table 1, we found that FI of the HiN fraction (0.61) was the lowest indicating that this fraction contained mostly allochthonous organic matter such as humic substances. HiB and HoB had the highest FI (2.23 and 2.60), indicating that these fraction contained mostly autochthonous organic matter, such as proteinaceous material. HiA and HoA had intermediate values of FI (1.33 and 1.30) and included both types of organic matter. In other research, SMP-like substances mainly included protein-like, tryptophan-like, and tyrosine-like compounds (*38*).

AAs as DCAcAm Precursors. Because protein-like, tryptophan-like, and tyrosine-like organic matter is made up of AAs, the DCAcAm yields of 20 AAs during chlorination were investigated (pH 7.5, AA concentration = 50 μmol/L, the molar ratio of chlorine as Cl to amino acids as N [Cl/N] = 4:1), as shown in SI Figure S8. Among the 7 AAs that could form DCAcAm above the detection limit (asparagine [Asn], aspartic acid [Asp], glutamine [Gln], histidine [His], phenylalanine, tryptophan [Trp], tyrosine [Tyr]), aspartic acid had the highest DCAcAm yield, followed by histidine. Interestingly, the AAs that formed DCAcAm in our study were similar to the ones that formed DCAN during chlorination, as reported by Ueno et al. (*39*) (SI Figure S8). It is quite likely that DCAcAm and DCAN share the same initial formation pathway, especially as hydrolysis of DCAN can form DCAcAm. Reckhow et al. (*15*) elaborated on the hydrolysis mechanism of DCAN, and we also discussed the formation of DCAcAm from aspartic acid in our pervious study (*33*). Here, we propose the main formation pathways of DCAcAm from the 7 AAs based on these previous studies (*15, 39*), as shown in eq 4 (where R-CH_2− represents the side chain in the AA). The initial

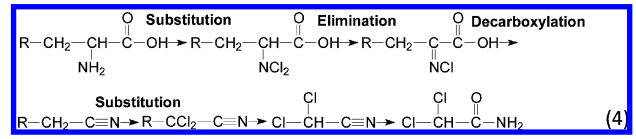

substitution, elimination, and decarboxylation reactions, and further substitution reaction to the methylene group (−CH_2−) of aspartic acid, tyrosine, and tryptophan have been reported by Trehy et al. (*35*). Theoretically, the 20 AAs all can follow the initial substitution, elimination, and decarboxylation reactions. The substitution reactions in the −CH_2− in the 20 AAs also occur, given that −CH_2− is an electron-donating group. However, the substitution reaction rates may be very different, due to the effect of R. The −CH_2− of 7 AAs (asparagine, aspartic acid, glutamine, histidine, phenylalanine, tryptophan, tyrosine) were easier to be substituted by chlorine than other AAs probably because of the R-enhanced electron-donating ability of −CH_2− of these AAs. Note that four of the AAs (histidine, phenylalanine, tyrosine, tryptophan) that form DCAcAm have aromatic rings as part of their R-groups.

Implications. Protein-like organic matter in certain hydrophilic fractions (HiA and HiB) played a critical role in DCAcAm formation. However, the conventional water treatment process (with coagulation, sedimentation, and filtration) or the use of activated carbon adsorption is more effective at removing the hydrophobic fractions. Therefore, enhanced treatment processes need to be considered for the hydrophilic fractions, especially protein-like organic matter. Total AA concentrations in natural waters are higher than free AA levels. Moreover, the reactivity of AAs to form DCAcAm in more complex structures may be different than that of the free AAs. Nonetheless, it is valuable to study free AAs as model compounds to investigate the DCAcAm formation mechanism.

Acknowledgments

This project was supported by the national major science and technology project of China (No. 2008ZX07421-002), "11th Five-year Plan" science and technology support project of China (No.2006BAJ08B06) and Shanghai Tongji Gao Tingyao Environmental Science & Technology Development Foundation. We thank Susan D. Richardson (USEPA) for helpful suggestions on HAcAm analysis. We also thank David A. Reckhow (University of Massachusetts) and Paul Westerhoff (Arizona State University) for helpful communications on N-DBPs.

Supporting Information Available

Table S1 shows the water quality of Qingcaosha Reservoir and the yields of DBPs during FP tests. Table S2 shows the DCAcAm yield of raw water and the weighted sum of the DCAcAm yields of each DOM fraction. Figure S1 shows molecular structural formulas of five of the identified HAcAms in drinking water. Figure S2 shows the fractionation pro-

cedure of the DOM. Figures S3 and S4 show the relationship between DCAN yields and DON/DOC, and DCAcAm yields and CF yields during chlorination in different months. Figure S5 shows the relationship between DCAcAm yields and DON/DOC during chlorination and chloramination of different DOM fractions. Figures S6 and S7 present fluorescence EEM spectra of DOM fractions, and a summary of the excitation and emission wavelength boundaries for five EEM regions. Figures S8 shows the DCAcAm yields of 20 AAs during chlorination. In addition, a brief description of the analytical method is provided. This material is available free of charge via the Internet at http://pubs.acs.org.

Literature Cited

(1) Rook, J. J. Formation of haloforms during chlorination of natural waters. *Water Treat. Exam.* **1974**, *23*, 234–243.

(2) Bellar, T. A.; Lichtenberg, J. J.; Kroner, R. C. The occurrence of organohalides in chlorinated drinking waters. *J. Am. Water Works Assoc.* **1974**, *66*, 703–706.

(3) Krasner, S. W.; McGuire, M. J.; Jacangelo, J. G.; Patania, N. L.; Reagan, K. W.; Aieta, E. M. The occurrence of disinfection by-products in US drinking water. *J. Am. Water Works Assoc.* **1989**, *81* (8), 41–53.

(4) Richardson, S. D.; Plewa, M. J.; Wagner, E. D.; Schoeny, R.; DeMarini, D. M. Occurrence, genotoxicity, and carcinogenicity of regulated and emerging disinfection by-products in drinking water: A review and roadmap for research. *Mutat. Res.* **2007**, *636* (1−3), 178–242.

(5) Sedlak, D. L.; Pinkston, K. E.; Gray, J. L.; Kolodziej, E. P. Approaches for quantifying the attenuation of wastewater-derived contaminants in the aquatic environment. *Chimia* **2003**, *57* (9), 567–569.

(6) Plewa, M. J.; Wagner, E. D.; Muellner, M. G.; Hsu, K. M.; Richardson, S. D. Comparative mammalian cell toxicity of N-DBPs and C-DBPs. In *Disinfection By-Products in Drinking Water: Occurrence, Formation, Health Effects and Control*; Karanfil, T., Krasner, S. W., Westerhoff, P., Xie, Y., Eds.; American Chemical Society: Washington, DC, 2008.

(7) Hua, G. H.; Reckhow, D. A. Determination of TOCl, TOBr and TOI in drinking water by pyrolysis and off-line ion chromatography. *Anal. Bioanal. Chem.* **2006**, *384* (2), 495–504.

(8) Krasner, S. W.; Weinberg, H. S.; Richardson, S. D.; Pastor, S. J.; Chinn, R.; Sclimenti, M. J.; Onstad, G. D.; Thruston, A. D., Jr. Occurrence of a new generation of disinfection byproducts. *Environ. Sci. Technol.* **2006**, *40* (23), 7175–7185.

(9) Chu, W. H.; Gao, N. Y.; Deng, Y.; Dong, B. Z. Formation of chloroform during chlorination of alanine in drinking water. *Chemosphere.* **2009**, *77* (10), 1346–1351.

(10) Liang, L.; Singer, P. C. Factors influencing the formation and relative distribution of haloacetic acids and trihalomethanes in drinking water. *Environ. Sci. Technol.* **2003**, *37* (13), 2920–2928.

(11) Pehlivanoglu-Mantas, E.; Sedlak, D. L. Wastewater-derived dissolved organic nitrogen: Analytical methods, characterization, and effects—A review. *Environ. Sci. Technol.* **2006**, *36* (3), 261–285.

(12) Muellner, M. G.; Wagner, E. D.; McCalla, K.; Richardson, S. D.; Woo, Y. T.; Plewa, M. J. Haloacetonitriles vs. regulated haloacetic acids: Are nitrogen-containing DBPs more toxic. *Environ. Sci. Technol.* **2007**, *41* (2), 645–651.

(13) Plewa, M. J.; Wagner, E. D.; Jazwierska, P.; Richardson, S. D.; Chen, P. H.; McKague, A. B. Halonitromethane drinking water disinfection byproducts: Chemical characterization and mammalian cell cytotoxicity and genotoxicity. *Environ. Sci. Technol.* **2004**, *38* (1), 62–68.

(14) Mitch, W. A.; Sedlak, D. L. Formation of *N*-nitrosodimethylamine (NDMA) from dimethylamine during chlorination. *Environ. Sci. Technol.* **2002**, *36* (4), 588–595.

(15) Reckhow, D. A.; Platt, T. L.; MacNeill, A. L.; McClellan, J. N. Formation and degradation of dichloroacetonitrile in drinking waters. *J. Water Supply Res. Technol.—Aqua* **2001**, *50* (1), 1–13.

(16) Lee, W.; Westerhoff, P.; Croue, J. P. Dissolved organic nitrogen as a precursor for chloroform, dichloroacetonitrile, N-nitrosodimethylamine, and trichloronitromethane. *Environ. Sci. Technol.* **2007**, *41* (15), 5485–5490.

(17) Krasner, S. W. The formation and control of emerging disinfection by-products of health concern. *Phil. Trans. R. Soc. A* **2009**, *367* (1904), 4077–4095.

(18) Plewa, M. J.; Muellner, M. G.; Richardson, S. D.; Fasano, F.; Buettner, K. M.; Woo, Y.-T.; McKague, A. B.; Wagner, E. D. Occurrence, synthesis, and mammalian cell cytotoxicity and genotoxicity of haloacetamides: An emerging class of nitrogenous drinking water disinfection byproducts. *Environ. Sci. Technol.* **2008**, *42* (3), 955–961.

(19) Westerhoff, P.; Mash, H. Dissolved organic nitrogen in drinking water supplies: A review. *J. Water Supply Res. Technol.—Aqua* **2002**, *51* (8), 415–448.

(20) Oliver, B. G. Dihaloacetonitriles in drinking water: Algae and fulvic acids as precursors. *Environ. Sci. Technol.* **1983**, *17* (2), 80–83.

(21) Leenheer, J. A. Comprehensive approach to preparative isolation and fractionation of dissolved organic carbon from natural waters and wastewaters. *Environ. Sci. Technol.* **1981**, *15* (5), 578–587.

(22) Imai, A.; Fukushima, T.; Matsushige, K.; Kim, Y. H.; Choi, K. Characterization of dissolved organic matter in effluents from wastewater treatment plants. *Water Res.* **2002**, *36* (4), 859–870.

(23) Zhang, H.; Qu, J. H.; Liu, H. J.; Zhao, X. Characterization of isolated fractions of dissolved organic matter from sewage treatment plant and the related disinfection by-products formation potential. *J. Hazard. Mater.* **2009**, *164* (2−3), 1433–1438.

(24) McKnight, D. M.; Boyer, E. W.; Westerhoff, P. K.; Doran, P. T.; Kulbe, T.; Andersen, D. T. Spectrofluorometric characterization of dissolved organic matter for indication of precursor organic material and aromaticity. *Limnol. Oceanogr.* **2001**, *46* (1), 38–48.

(25) Krasner, S. W.; Sclimenti, M. J.; Guo, Y. C.; Hwang, C. J.; Westerhoff, P. Development of DBP and nitrosamine formation potential tests for treated wastewater, reclaimed water, and drinking water. *Proceedings of the 2004 AWWA Water Quality Technology Conference*; AWWA: Denver, CO, 2004.

(26) Krasner, S. W.; Sclimenti, M. J.; Mitch, W.; Westerhoff, P.; Dotson, A. Using formation potential tests to elucidate the reactivity of DBP precursors with chlorine versus with chloramines. *Proceedings of the 2007 AWWA Water Quality Technology Conference*; AWWA: Denver, CO, 2007.

(27) Dotson, A.; Westerhoff, P.; Krasner, S. W. Nitrogen enriched dissolved organic matter (DOM) isolates and their affinity to form emerging disinfection by-products. *Water Sci. Technol.* **2009**, *60* (1), 135–143.

(28) Li, C. W.; Korshin, G. V.; Benjamin, M. M. Monitoring DBP formation with differential UV spectroscopy. *J. Am. Water Works Assoc.* **1998**, *90* (8), 88–100.

(29) Li, C. W.; Benjamin, M. M.; Korshin, G. V. Use of UV spectroscopy to characterize the reaction between NOM and free chlorine. *Environ. Sci. Technol.* **2000**, *34* (12), 2570–2575.

(30) Greenberg, A. E.; Clesceri, L. S.; Eaton, A. D., Eds. *Standard Methods for the Examination of Water and Wastewater*, 20th ed.; APHA, AWWA, WEF: Washington, DC, 1998.

(31) Chu, W. H.; Gao, N. Y.; Deng, Y. Stability of newfound nitrogenous disinfection by-products: Haloacetamides in drinking water. *Chin. J. Org. Chem.* **2009**, *29* (10), 1569–1574.

(32) Chu, W. H.; Gao, N. Y. Determination of nitrogenous disinfection byproducts: Chloroacetamides in drinking water by gas chromatography-mass spectrometry. *Chin. J. Anal. Chem.* **2009**, *37* (1), 103–106.

(33) Chu, W. H.; Gao, N. Y.; Deng, Y. Formation of haloacetamides during chlorination of dissolved organic nitrogen aspartic acid. *J. Hazard. Mater.* **2010**, *173* (1−3), 82–86.

(34) Reckhow, D. A.; Singer, P. C.; Malcolm, R. L. Chlorination of humic materials—By-product formation and chemical interpretations. *Environ. Sci. Technol.* **1990**, *24* (11), 1655–1664.

(35) Trehy, M. L.; Yost, R. A.; Miles, C. J. Chlorination byproducts of amino acids in natural waters. *Environ. Sci. Technol.* **1986**, *20* (11), 1117–1122.

(36) Krasner, S. W.; Croue, J. P.; Buffle, J.; Perdue, E. M. Three approaches for characterizing NOM. *J. Am. Water Works Assoc.* **1996**, *88* (6), 66–79.

(37) Nikolaou, A. D.; Lekkas, T. D. The role of natural organic matter during formation of chlorination by-products: A review. *Acta Hydrochim. Hydrobiol.* **2001**, *29* (2−3), 63–77.

(38) Chen, W.; Westerhoff, P.; Leenheer, J. A.; Booksh, K. Fluorescence excitation - emission matrix regional integration to quantify spectra for dissolved organic matter. *Environ. Sci. Technol.* **2003**, *37* (24), 5701–5710.

(39) Ueno, H.; Moto, T.; Sayato, Y.; Nakamuro, K. Disinfection by-products in the chlorination of organic nitrogen compounds: By-products from kynurenine. *Chemosphere.* **1996**, *33* (8), 1425–1433.

ES100397X